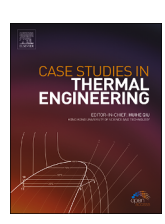
FISEVIER

Contents lists available at ScienceDirect

## Case Studies in Thermal Engineering

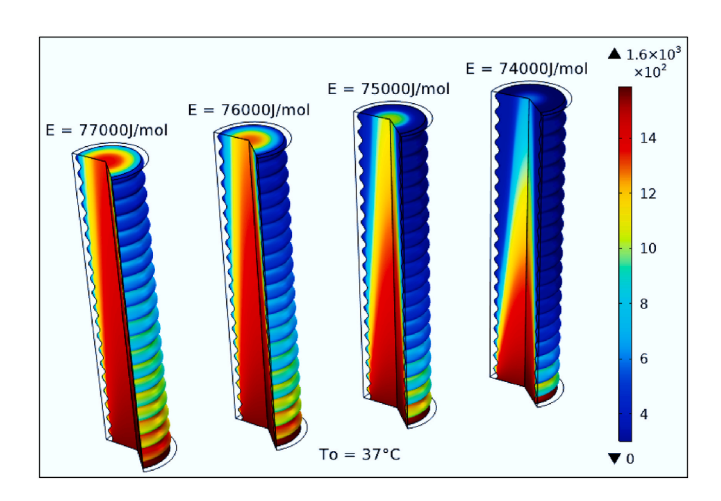
journal homepage: www.elsevier.com/locate/csite



# CFD-aided enhancement of propylene oxide decomposition in a tubular reactor with a corrugated cooling jacket

Djelloul Bendaho <sup>a</sup>, Noureddine Kaid <sup>b</sup>, Sultan Alqahtani <sup>c</sup>, Badr M. Alshammari <sup>d</sup>, Younes Menni <sup>b</sup>, <sup>e</sup>, <sup>f</sup>, <sup>\*</sup>, Ali J. Chamkha <sup>g</sup>, <sup>\*\*</sup>, Lioua Kolsi <sup>h</sup>

### GRAPHICAL ABSTRACT



E-mail addresses: menni.younes@cuniv-naama.dz (Y. Menni), achamkha@yahoo.com (A.J. Chamkha).

https://doi.org/10.1016/j.csite.2024.105004

Received 24 April 2024; Received in revised form 28 July 2024; Accepted 18 August 2024

Available online 19 August 2024

2214-157X/© 2024 The Authors. Published by Elsevier Ltd. This is an open access article under the CC BY-NC-ND license (http://creativecommons.org/licenses/by-nc-nd/4.0/).

a Institute of Technology, University Center Salhi Ahmed Naama (Ctr. Univ. Naama), P.O. Box 66, Naama, 45000, Algeria

b Energy and Environment Laboratory, Department of Mechanical Engineering, Institute of Technology, University Center Salhi Ahmed Naama (Ctr. Univ. Naama), P.O. Box 66, Naama, 45000, Algeria

<sup>&</sup>lt;sup>c</sup> College of Engineering, Mechanical Engineering Department, King Khalid University, Abha, Saudi Arabia

d Department of Electrical Engineering, College of Engineering, University of Ha'il, Ha'il City, 81451, Saudi Arabia

<sup>&</sup>lt;sup>e</sup> College of Technical Engineering, National University of Science and Technology, Dhi Qar, 64001, Iraq

<sup>&</sup>lt;sup>f</sup> Faculty of Engineering and Natural Sciences, Biruni University, Topkapi, Istanbul, Turkey

g Faculty of Engineering, Kuwait College of Science and Technology, Doha District, 35004, Kuwait

h Department of Mechanical Engineering, College of Engineering, University of Ha'il, Ha'il City, 81451, Saudi Arabia

<sup>\*</sup> Corresponding author. Energy and Environment Laboratory, Department of Mechanical Engineering, Institute of Technology, University Center Salhi Ahmed Naama (Ctr. Univ. Naama), P.O. Box 66, Naama, 45000, Algeria.

<sup>\*\*</sup> Corresponding author.

#### ARTICLE INFO

Keywords:
Propylene oxide
Decomposition kinetics
Reactor design
CFD
Activation energy
Heat transfer

#### ABSTRACT

This research delves into the decomposition kinetics of propylene oxide within a novel reactor design characterized by a corrugated inner wall for enhanced cooling. By applying Computational Fluid Dynamics (CFD), this study aims to optimize the reactor's heat transfer capabilities to achieve precise control over the exothermic decomposition process. This approach addresses a previously unexplored area in CFD application, proposing a model that fine-tunes the decomposition efficiency of propylene oxide by considering the interplay of key parameters such as inlet mixture temperature, activation energy, flow rate, and the resulting thermal profile. The primary goal is to advance the development of more efficient and environmentally friendly chemical processing techniques in the propylene oxide industry. The study highlights the critical relationship between activation energy (74-76 kJ/mol), process temperature (29-37 °C), and cooling efficiency in optimizing the decomposition process. Significant findings indicate that higher inlet temperatures (37 °C) and lower activation energies (74 kJ/mol) lead to superior conversion rates. The study presents a clear correlation between temperature elevation, reduced activation energy, and enhanced conversion rates, demonstrating that optimizing these parameters can lead to significantly improved conversion efficiencies, potentially approaching 100 % under ideal conditions.

#### 1. Introduction

Computational Fluid Dynamics (CFD) has assumed a pivotal role in examining chemically reacting flows, witnessing a substantial surge in adoption. While it is well-established for investigating single-phase reactor configurations, such as agitated vessels and void-containing conduits, its extension to multiphase reactor systems, including fixed beds, bubble columns, trickle beds, and fluidized beds, remains nascent and characterized by initial development and refinement [1].

In the field of a packed tubular reactor, the conservation equations are formulated by accounting for variations in axial velocity across the radius, radial diffusion rates, and radial thermal conductivity. These parameters are crucial components of the mathemati-

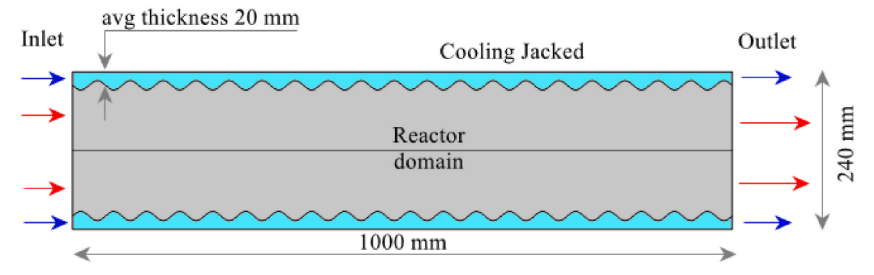


Fig. 1. Reactor characteristics.

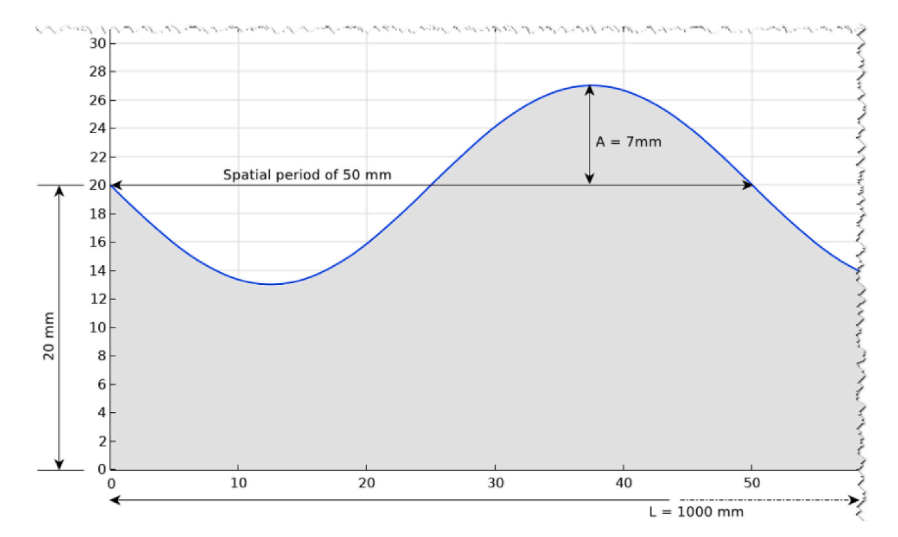


Fig. 2. Dimensions and shape of the internal corrugated jacket wall. The corrugated internal surface increases the contact area with the fluid to enhance heat transfer.

(a)

Fig. 3. Axisymmetric geometry model of the reactor with corrugated internal jacket wall.

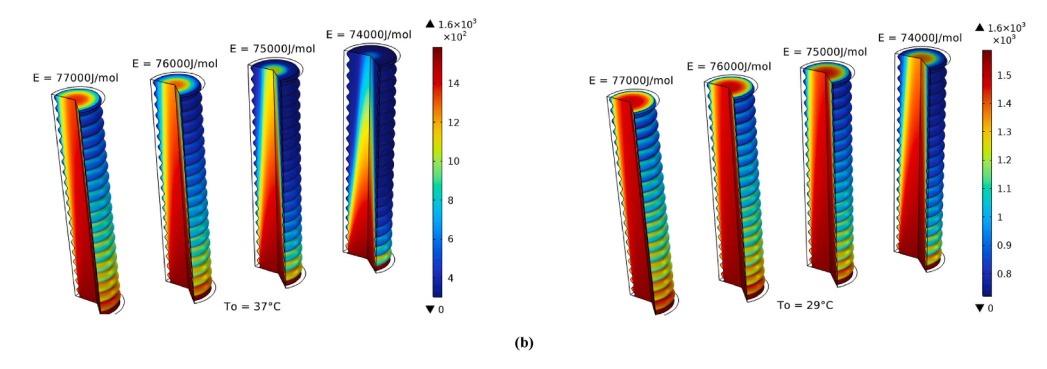


Fig. 4. Propylene oxide decomposition vs energy activation at (a) 37 °C and (b) 29 °C.

cal model. By applying these relationships, profiles for radial diffusivity and thermal conductivity are derived, providing valuable insights into the transport phenomena within the reactor system. This analytical approach facilitates a detailed understanding of the intricate dynamics governing the reactor's performance [2].

In the complex domain of tubular reactors dealing with viscous flows, a thorough investigation is conducted into the intricate orchestration of chemical reactions. The focus is on the subtle interplay between localized and overall conversion rates, while considering the nuances of radial diffusion and the dynamic distribution of reaction times across the radial spectrum. This effort aims not only to elucidate the behavior of first-order reactions across a wide range of dimensionless variables but also to develop precise mathematical expressions that reveal the critical points where diffusion becomes negligible. This approach provides a clearer understanding of its role, or lack thereof, in shaping the reactor's overall performance [3].

The urgent need to address ongoing environmental degradation and contamination caused by reliance on fossil fuels serves as a compelling catalyst for the increased adoption of renewable energy sources. Adapting reactor technologies, particularly tubular reactors, is a crucial strategy for enhancing, commercializing, and expanding the use of biodiesel. This transition aligns with the goal of environmental sustainability and highlights the importance of technological innovation in addressing pressing global energy challenges [4].

Collision theory states that for a chemical reaction to happen, reactant molecules must collide with enough energy and the right orientation. This helps them overcome the activation energy barrier and turn into products. The theory highlights the essential role of molecular collisions in initiating and driving chemical reactions, offering valuable insights into reaction kinetics and mechanisms [5–7].

In large-scale industrial applications, facilities are often located on the outskirts to accommodate the spatial requirements of these operations. One significant compound of interest in this context is epoxy propane, commonly known as propylene oxide. This chemical compound is extensively used in chemical reactions during intermediate stages of production. Its widespread application within the chemical industry is crucial for generating commercially viable products. Remarkably, epoxy propane is among a select group of 50 compounds regularly employed in essential manufacturing processes, highlighting its substantial industrial significance. Additionally, there has been a notable surge in annual demand for this compound, reaching up to 14 billion pounds, further emphasizing its pivotal role in contemporary industrial processes [8].

Propylene glycol, an essential additive in the food industry, is synthesized from propylene oxide and water. It performs various functions, such as strengthening dough, preserving moisture, and acting as an emulsifier and texturizer. Providing adequate activation energy to reactants is crucial for achieving desired yields and properties, aligning with both research objectives and industrial processes [9–11].

The thermal distribution in reactors heavily depends on the thermal conductivity of the chemical mixture or base fluid [12–15]. Additionally, the diffusion of chemical species within the reactor significantly affects the reaction rate. Therefore, optimizing thermal and mass transfer parameters is essential in modern engineering industries [16–18].

Das et al. [19] investigated how a reaction following first-order kinetics, occurring in a homogeneous medium, affects an unsteady flow while maintaining a uniform distribution of mass and heat. Their analysis employed a setup with an infinite vertical plate as the focal point of examination. In a related study, Brown & Lai [20] numerically analyzed the transfer of heat and mass in a vertically oriented cavity subjected to heating from below. To enhance understanding in this field, they established correlations between non-dimensional parameters related to dynamics and thermal characteristics. Following these studies, Parvin et al. [21] examined double-diffusive effects by employing Soret and Dufour coefficients within an enclosed space subjected to heating, utilizing Al<sub>2</sub>O<sub>3</sub>-H<sub>2</sub>O nanofluids. Additionally, other research explored the effects of chemical reactions and radiation on unsteady flows involving magne-

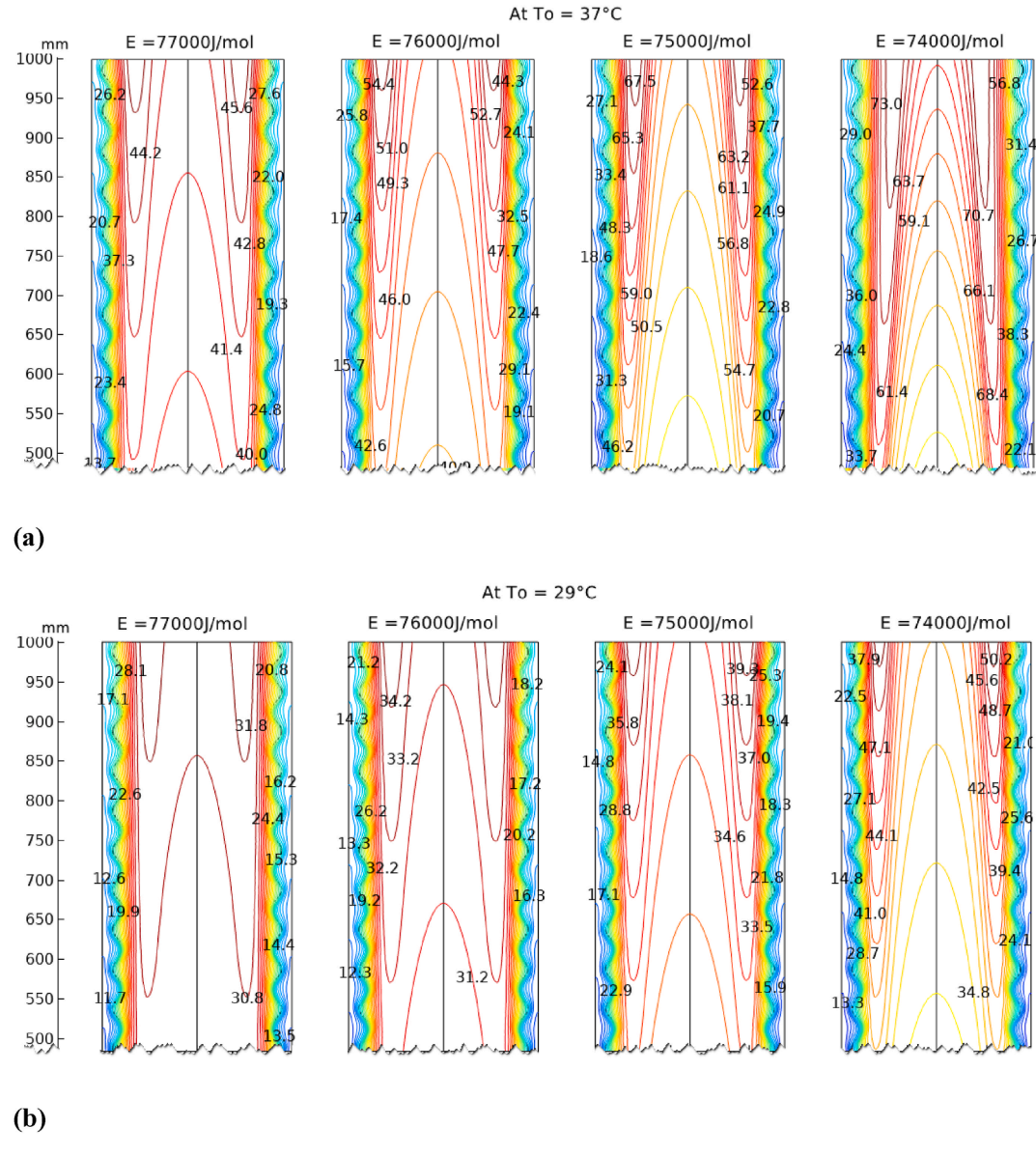
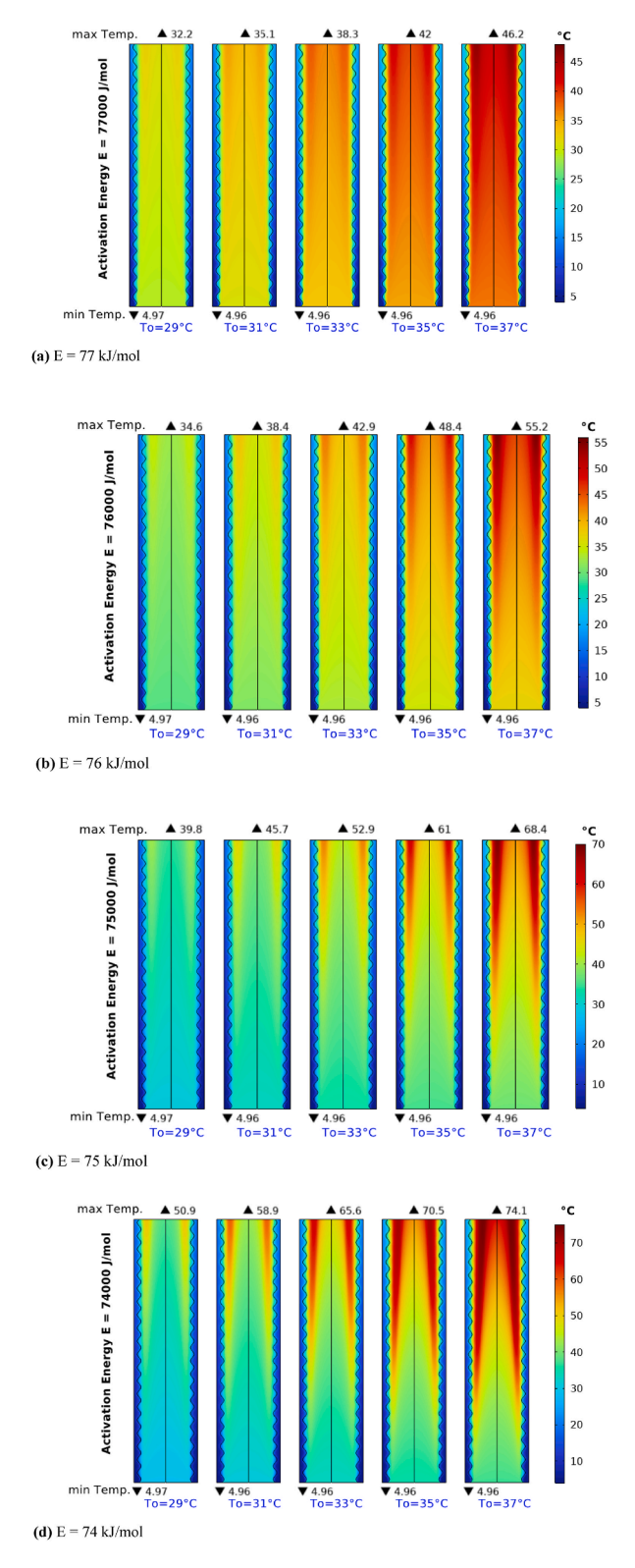


Fig. 5. Isothermal contour of the reactor and cooling jacket near the outlet at (a) 37 °C and (b) 29 °C.

tohydrodynamics (MHD) and free convection. Specifically, these studies focused on the flow around a semi-infinite plate in motion, influenced by either the presence of a heat source or suction. Collectively, these investigations aimed to provide significant insights into the dynamic interplay of these phenomena [22–26].

Hayat et al. [27] examined the effects of homogeneous-heterogeneous reactions in nanofluid flow over a non-linear stretching sheet, using OHAM for solution convergence. Ribert et al. [28] developed a numerical model for counterflow diffusion flames across different fluid thermodynamic states. Bachok et al. [29] studied homogeneous-heterogeneous reactions in boundary layer flow near a stretching surface. Frolov et al. [30] presented a model for catalytic monomethylaniline synthesis, proposing an optimal control method. Masoumi et al. [31] designed a pilot plant to study furnace parameter effects on reactor yields. Logtenberg & Dixon [32] used CFD to simulate heat transfer in a packed bed reactor. Additional studies by Kusumastuti et al. [33], Nailwal et al. [34], and Wu et al. [35] further explored fluid dynamics and heat transfer in various applications, enriching the field's knowledge base.

This comprehensive literature review provides invaluable insights into heat transfer, mass transfer, and fluid dynamics across diverse reactor configurations. Such knowledge is a crucial foundation in the continuous effort to refine and optimize reactor designs and processes, promising efficient production of a wide range of industrial products. The synthesis of this research aids in advancing sustainable and technologically driven solutions within chemical engineering. This study specifically aims to optimize the decomposition of propylene oxide within a corrugated inner cooling jacket tubular reactor. By parametrically analyzing the influence of mixture inlet temperature, activation energy, and inlet flow rate on decomposition percentage, the study ensures safe and efficient operation.



 $\textbf{Fig. 6.} \ \textbf{Surface temperature for different inlet temperatures and activation energies.}$ 

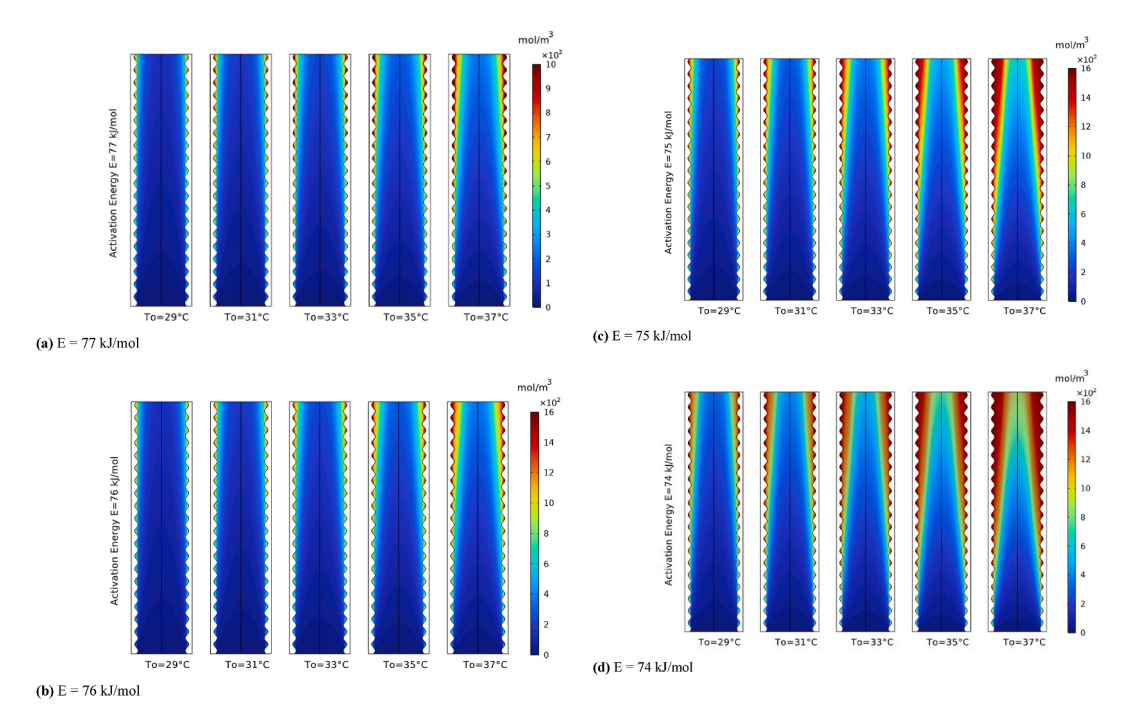


Fig. 7. Conversion surface of produced Propylene glycol for different inlet temperatures and activation energies.

The primary objective is to maximize decomposition while maintaining the peak exothermic temperature below 75 °C, thereby evaluating the effectiveness of the corrugated cooling jacket design in achieving thermal control and contributing to overall process optimization.

## 2. Mathematical modeling

Propylene glycol (PG) is obtained through a liquid-phase hydrolytic process from propylene oxide (PO). Using excess water and a catalytic amount of sulfuric acid, the reaction proceeds at moderate temperatures. However, significant exothermic heating necessitates the use of a large water excess for optimal temperature control.

Methanol was added to address the limited miscibility between propylene oxide and water. The behavior of the resulting non-ideal mixture was successfully modeled using the Non-Random Two-Liquid (NRTL) equation.

The NRTL equation is a thermodynamic model used to describe the non-ideal behavior of liquid mixtures. It is particularly useful for systems with significant deviations from ideal behavior, such as hydrogen bonding, solvation effects, or other strong intermolecular interactions. In this study.

- Propylene oxide is a polar, aprotic solvent that can interact with the polar water and methanol molecules through dipole-dipole interactions and hydrogen bonding.
- Water and methanol are polar, protic solvents that can form strong hydrogen bonds with each other, as well as with propylene oxide.

The NRTL equation was selected to model the propylene oxide, water, and methanol system because it is well-equipped to account for the significant non-ideal interactions between these components.

The reaction rate exhibited a power-law dependence on propylene oxide concentration, highlighting the importance of precise feedstock control for efficient production. A corrugated cooling jacket reactor was used to limit the peak temperature produced by the exothermic reaction while achieving complete PO conversion (see Fig. 1).

The corrugation is a sinusoidal function applied along the length of the reactor L = 1000 mm,

$$y(z) = A \cos(2\pi f z + \varphi) = A \cos\left(2\pi \frac{1}{50}z + \frac{\pi}{2}\right)$$
 (1)

Where.

A is the amplitude,

z, the independent variable, represents space in millimeters (ranging from 0 to L),

f represents the number of complete cycles or oscillations within 1 mm, and

 $\varphi$  represents the angular position or the specific point in the oscillation cycle at the initial space z=0 (see Fig. 2).

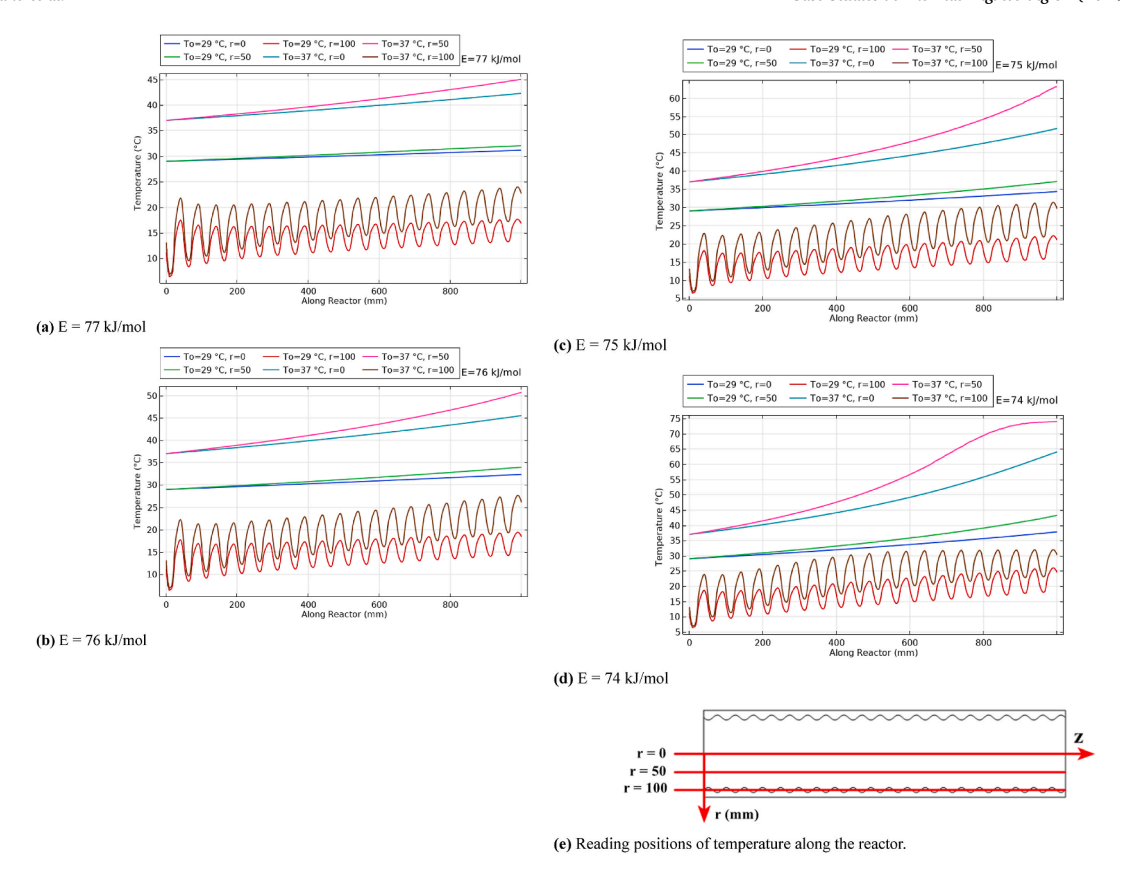


Fig. 8. Axial temperature along the reactor in three positions (see Fig. 7(e)), where the inlet temperatures are 29 °C and 37 °C, and different activation energies are used.

#### 2.1. Reaction

Under different conditions, propylene oxide ( $C_3H_6O$ ) can undergo decomposition through various mechanisms. Two representative reactions involve the breakdown of propylene oxide:

- Thermal decomposition: Propylene oxide exhibits thermal decomposition at elevated temperatures, yielding carbon dioxide  $CO_2$  and propylene  $C_3H_6$ .

$$C_3H_6O \rightarrow C_3H_6 + CO_2 \tag{2}$$

- Acid-catalyzed decomposition: In acidic environments, propylene oxide is susceptible to acid-catalyzed decomposition, leading to the formation of propanol  $C_3H_8O$  and water  $H_2O$ . Typically, an acid catalyst, such as  $H_2SO_4$  (sulfuric acid) or  $H_3PO_4$  (phosphoric acid), is employed to enhance the reaction rate in this process.

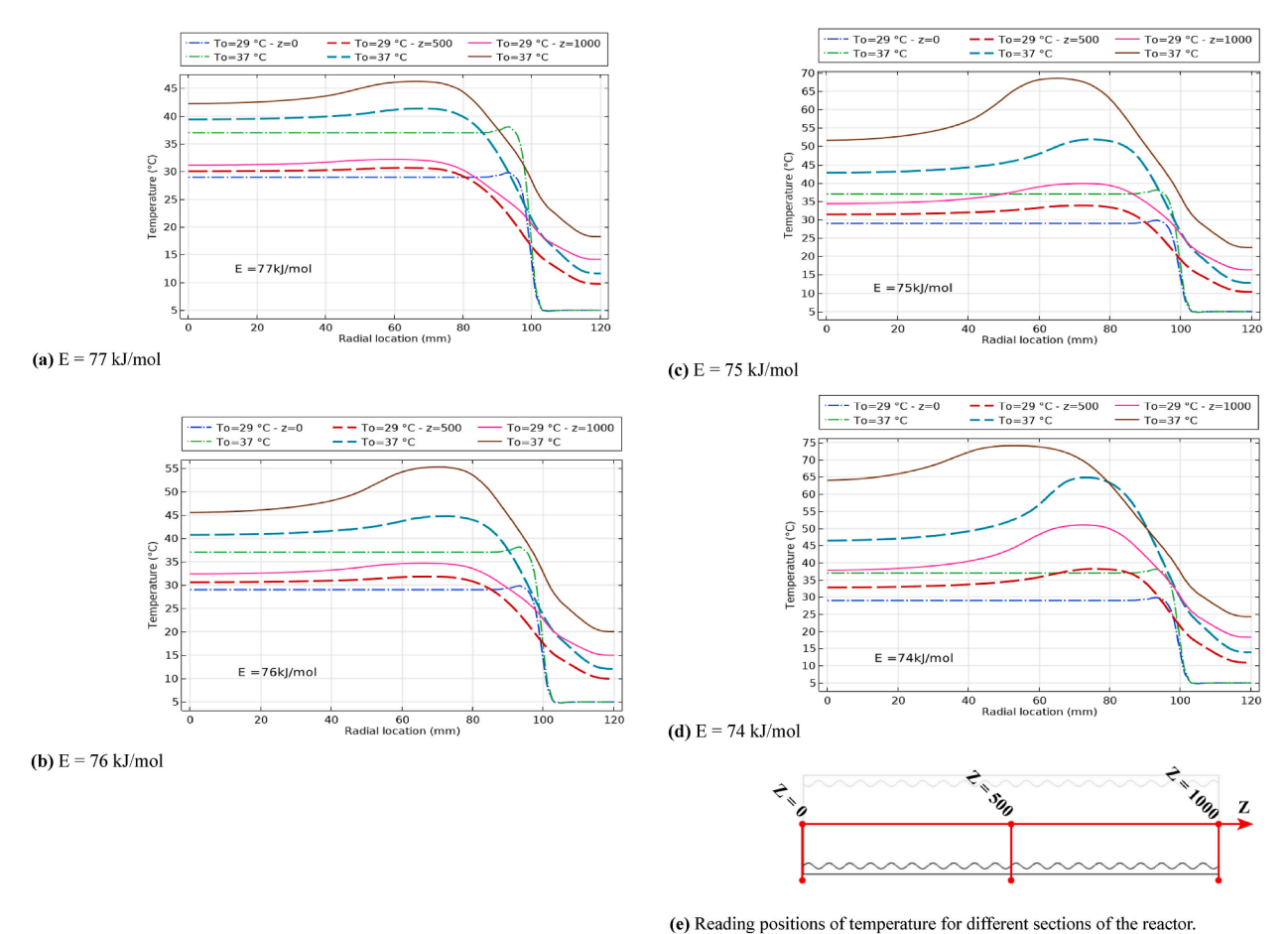
$$C_3H_6O + H_2O \rightarrow C_3H_8O + H_2O$$
 (3)

Propylene oxide serves a crucial role in the synthesis of propylene glycol, a versatile chemical with widespread applications in industries such as cosmetics, pharmaceuticals, food, and beverage, and automotive. Propylene glycol functions as a solvent, emulsifier, and humectant, contributing to various products including lotions, creams, medicines, antifreeze, and food additives.

$$C_3H_6O + H_2O \xrightarrow{CH_3OH} C_3H_8O_2 \tag{4}$$

In the context of exothermic reactions, this particular process unfolds as a first-order reaction, especially notable given its execution in an environment of plentiful water. The reactor's intake is characterized by a bifurcated flow. One stream comprises an equimolar blend of  $C_3H_6O$  and methanol, while the other carries water with 0.1 % sulfuric acid by weight added. The fusion of these streams triggers an immediate surge in temperature, a manifestation of the mixture's inherent heat. In our computations, this thermal elevation is duly considered, with the inlet temperatures of both streams carefully set within the range of 29 °C–37 °C.

The kinetics of a first-order exothermic decomposition reaction can be described using the Arrhenius equation, which relates the reaction rate constant *k* to temperature. The general form of the first-order reaction rate formula is:



.

$$k = k_0 e^{\left(-E/RT\right)} \tag{5}$$

Fig. 9. Temperature profiles at different sections of the reactor (see Fig. 9(e)) vs activation energy.

Where.

 $k_0$  is the pre-exponential factor, and E is the activation energy.

The  $k_0$  rate in the Arrhenius equation (5) is typically determined experimentally through kinetic studies. The experiment is repeated at different temperatures, and the reaction rate is measured over time using methods such as spectrophotometry, chromatography, or titration. The reaction rate versus temperature is plotted, and the reaction rate constant  $k_0$  is determined from the data.

The activation energy E is measured in the same units as RT, falls within the range of 74,000 to 77,000 J/mol, with R representing the universal gas constant (8.314 J/(mol·K)). This can also be expressed as:

$$k(T) = k_0(T_0) \cdot exp\left[\frac{E}{R}\left(\frac{1}{T_0} - \frac{1}{T}\right)\right]$$
(6)

Where.

k(T) is the reaction rate constant at temperature,

 $k_0(T_0)$  is the reaction rate constant at the reference temperature,

T is the temperature at which the reaction rate constant is being evaluated, and

 $T_0$  is the reference temperature.

## 2.2. Geometry

Leveraging the insights from Fig. 3's graphical representation of the model's geometric layout, we proceed with precision by assuming negligible angular variations around the central axis, thus treating the model as axisymmetric. This foundational understanding guides our computational approach as we explore the system's intricacies, represented by a comprehensive set of equations on a

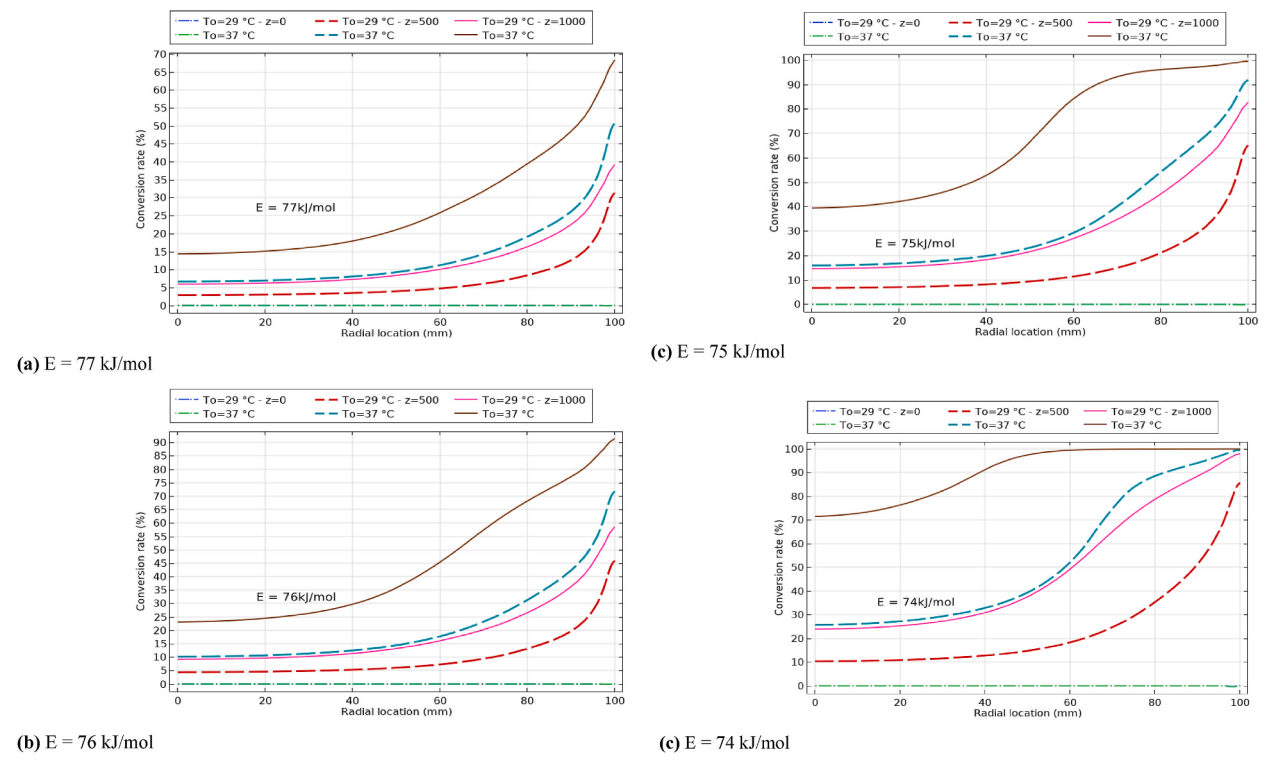


Fig. 10. Reaction conversion rate (%) at different sections of the reactor (see Fig. 9(e)) vs activation energy.

2D plane. The delineated boundaries in the rz plane accurately depict the essential components of the cylindrical reactor, including the inflow and outflow sections, reactor wall, and central axis, each contributing distinctly to the system's structural integrity.

Under the assumption of uniform diffusivity across all three species, our approach entails modeling the reactor using three distinct differential equations: one for the mass balance of a selected species (with the understanding that mass balances for the remaining two species are redundant, as explained in subsequent sections), another for thermal equilibrium within the reactor core, and a third for the thermal equilibrium of the heating jacket.

## 2.3. Model equations

In delineating the operational dynamics of the reactor, a crucial framework is established through the governing equations that encapsulate material and energy balance within its confines. These equations are intricately defined with respect to two distinct variables: the radial dimension r and the axial dimension z. Together, they form a system of two coupled partial differential equations, describing the behavior of the reactor across both spatial dimensions. Central to this system is the equation governing the conservation of mass, which serves as a key element for understanding the intricate interplay of substances within the reactor.

## 2.3.1. Mass balance for species A

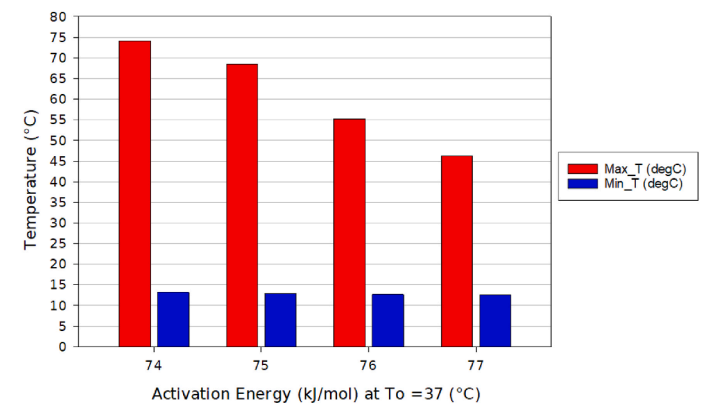
$$D_P \frac{1}{r} \frac{\partial C_A}{\partial r} + D_P \frac{\partial^2 C_A}{\partial r^2} + D_P \frac{\partial^2 C_A}{\partial z^2} - 2U \left( 1 - \left( \frac{r}{R_a} \right)^2 \right) \frac{\partial C_A}{\partial z} + r_A = 0 \tag{7}$$

In the above equation,  $D_P$  governs diffusion,  $C_A$  represents concentration, U steers velocity,  $R_a$  defines radius, and  $\partial r$  is the rate of reaction.

## 2.3.2. Reactor internal energy balance

$$k\frac{1}{r}\frac{\partial T}{\partial r} + k\frac{\partial^2 T}{\partial r^2} + k\frac{\partial^2 T}{\partial z^2} - 2U\left(1 - \left(\frac{r}{R_a}\right)^2\right)\rho C_P \frac{\partial T}{\partial z} - r_A\left(-\Delta H_{Rx}\right)$$
(8)

Within this investigation, we operate under the presumption that species A, B, and C share identical diffusivity properties, thereby streamlining our focus to solving a single material balance equation. Our understanding of the concentrations of other species is facilitated by the principles of stoichiometry.



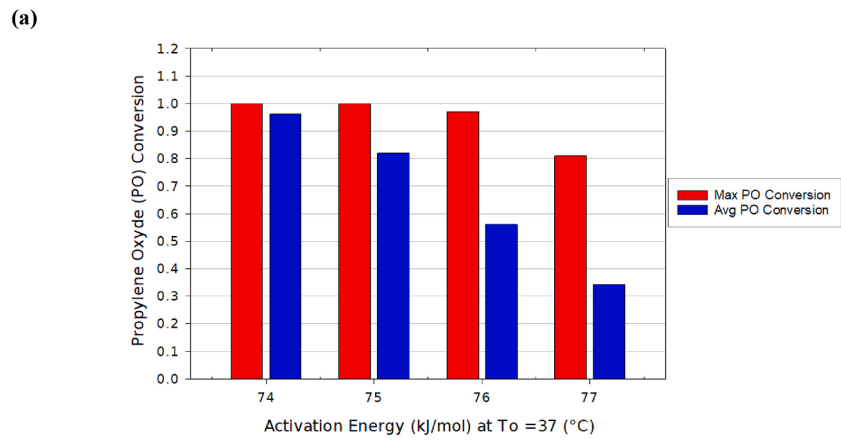


Fig. 11. (a) Maximum and minimum temperatures, (b) Maximum and average propylene oxide conversion at  $T_0=37\,^{\circ}\mathrm{C}$  for different activation energies.

## 2.4. Boundary conditions

## 2.4.1. Boundary conditions for mass balance

**(b)** 

• Entry (z = 0):

$$C_A(r,0) = C_{A0} \tag{9}$$

- On the wall (r = R):

$$\frac{\partial C_A}{\partial r}(R, z) = 0 \tag{10}$$

The outlet boundary condition selected highlights the prevalence of convection in transporting substances out of the reactor. By maintaining an open outlet boundary, it refrains from constraining concentration levels.

## 2.4.2. Boundary conditions for energy balance

• Inlet (z = 0)

$$T(r,0) = T_0 (11)$$

- Outlet (z = L)

$$-\frac{\partial T}{\partial r}(r,L) = 0 \tag{12}$$

• On the wall (r = R)

$$-\frac{\partial T}{\partial r}(R,z) = \frac{U_K}{K} \left( T - T_a \right) \tag{13}$$

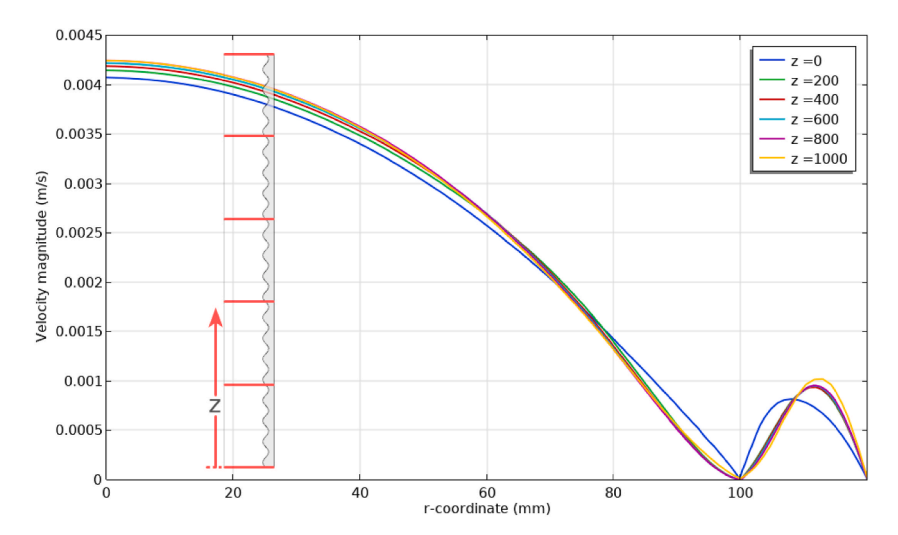


Fig. 12. Velocity profile of fluid in the cylindrical reactor at various axial positions.

Where, the variable L represents its length,  $U_K$  is an overall heat transfer coefficient, while K denotes thermal conductivity. The density is symbolized by  $\rho$ , and  $C_P$  stands for heating capacity. Additionally, the symbol  $\Delta$ HRx represents the enthalpy of reaction within this system.

#### 2.5. Assumptions

Within the reactor, the axial diffusion/dispersion flux of species A is considered negligible compared to the convective flux. When summing the enthalpy terms in the energy balance equation, the product of heat capacity and velocity ( $C_p \times U$ ) is treated as a combined heat capacity flux for each species.

The analysis focuses on a system that has reached a constant state, where the concentrations, temperatures, and other properties remain unchanged over time.

#### 3. Results and discussion

The effect of activation energy on the rate of decomposition is inversely proportional. Higher activation energies (above 74,000 J/mol) slow the reaction, requiring more energy for molecules to overcome the barrier. However, below this value, the behavior diverges. The original decomposition pathway might become unfavorable, leading to alternative reaction pathways that produce different components. This deviation can significantly increase the reaction rate beyond predictions based on the main decomposition pathway.

Higher temperatures generally accelerate the decomposition process in the designated pathway, but they also become a double-edged sword in this context. At higher temperatures (see Fig. 4(a)), more molecules can be activated for the intended decomposition, but they can also trigger an undesirable divergent reaction. Conversely, at low inlet temperatures (see Fig. 4(b)), the conversion of PO is insufficient.

The undesirable divergent reaction is an uncontrolled, rapid decomposition reaction that can generate large amounts of heat and pressure, potentially causing equipment failure and explosions, posing serious safety risks.

Fig. 5(a) presents isothermal contours within a reactor and its cooling jacket for varying activation energies. The reactor inlet temperature is maintained at 37 °C, while the cooling water inlet temperature is fixed at 5 °C. Analyzing the contours across different activation energies allows us to understand the reactor's thermal behavior and the effectiveness of the cooling jacket.

The contours reveal a non-uniform temperature distribution within the reactor, with hotter regions concentrated near the cooling zone and the center of the reactor. This is consistent with the exothermic nature of the reaction. As the activation energy increases (moving from left to right in the figure), the overall temperature within the reactor generally rises. The presence of the cooling jacket helps maintain lower temperatures near the reactor walls compared to the core region. This temperature gradient is crucial for efficient heat removal and preventing the reactor from overheating. It has been observed that a decrease in the inlet temperature to 29 °C is directly correlated with a decrease in the rate of the overall decomposition reaction. It also leads to unwanted propylene glycol production as a byproduct, as seen in Fig. 5(b).

The control of the decomposition reaction of propylene oxide within the reactor featuring a corrugated cooling wall is achieved while ensuring that the critical temperature threshold of 75  $^{\circ}$ C, denoted as the critical temperature of the reaction, is not surpassed.

Fig. 6(a–d) illustrates the temperatures observed at the reactor outlet under varying conditions, including different inlet temperatures of propylene oxide with its catalyst and diverse values of the activation energy (*E*). In instances where a high activation energy value of 77,000 J/mol is employed, a moderate temperature increase is discerned, and the temperature distribution remains relatively uniform along the reactor.

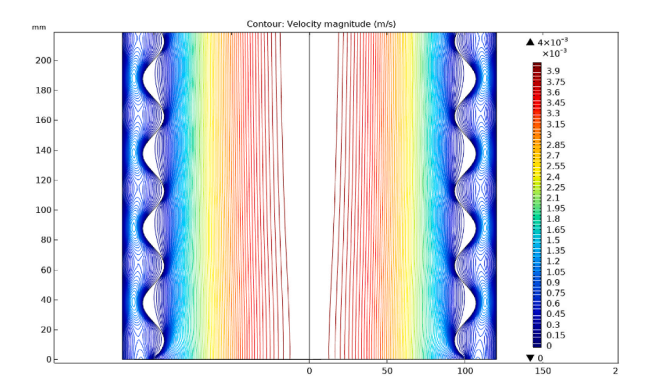


Fig. 13. Velocity magnitude contour across the reactor.

Conversely, when an activation energy of 74,000 J/mol is used, the temperature rises quickly due to the exothermic nature of the reaction. This temperature increase is especially noticeable at the reactor outlet.

These observations indicate a direct correlation between temperature levels and the extent of conversion, with lower temperatures corresponding to minimal conversion, and conversely, higher temperatures associated with increased conversion, as seen from the Propylene glycol conversion in Fig. 7(a–d). This dependency is due to how temperature affects the reaction rate. Specifically, the lower temperatures near the reactor wall are caused by the cooling effect of the coolant in that area.

Fig. 8(a–d) presents detailed curves showing the temperature distribution within the non-isothermal reactor. These curves highlight the crucial role of the cooling jacket in effectively managing the heat generated by the reaction, thereby maintaining the desired temperature profile. At r=100, the curve intersects the corrugated inner wall of the cooling jacket, indicating the direct influence of the cooling medium on temperature regulation. Notably, at the axial position r=0, where the velocity is maximal, the reaction does not have enough time to complete. Due to the exothermic nature of the reaction, this limited reaction time results in insufficient energy production, leading to a noticeable decrease in temperature. In the intermediate range (r=50), the reaction has more time to progress, producing increased energy and more propylene glycol (see Fig. 7). Consequently, this extended reaction time leads to a significant rise in temperature.

Fig. 9(a–d) shows the temperature and conversion surface profiles at three distinct locations (see Fig. 9(e)) along the length of the reactor. As the reactants move through the reactor, a clear trend emerges: the intensity of the reaction increases, leading to a corresponding rise in temperature. The influence of the coolant on these profiles is also evident, highlighting its impact on the observed temperature variations. The temperature evolution reveals important trends in the reactor's thermal performance. Specifically, with an initial temperature of 29 °C (302K) and a constant activation energy of 74 kJ/mol, the temperature at the reactor outlet reached 38 °C (311K). In contrast, with an initial temperature of 37 °C (312K) under the same activation energy conditions, the temperature at the reactor's end rose substantially to 74 °C (347K). This significant temperature increase underscores the exothermic nature of the reaction, indicating substantial heat liberation during the process. The variations in reactor temperature, under different initial conditions and activation energy settings, affect the mean temperature within the cooling jacket, which rises to 30 °C. This temperature increase is attributed to the heat transfer between the reactor and the cooling jacket.

Achieving complete conversion, represented by 100 %, indicates that every molecule of propylene oxide within the system has been fully transformed into propylene glycol at a specific point in time. This signifies the exhaustive consumption of the reactant and the formation of the desired product.

In Fig. 10(a–d), it is evident that with an elevated activation energy of E = 77 kJ/mol, the conversion rate peaks at 70 %. In contrast, a lower activation energy of E = 74 kJ/mol results in a significant increase in the conversion rate, reaching 100 %. The higher speed at the reactor center limits the residence time, preventing a substantial increase in conversion. However, closer to the corrugated wall, where the flow rate decreases and the conversion rate rises due to sustained high temperatures, the reaction rate is enhanced.

Approaching the wavy wall, the conversion remains constant compared to the smooth wall. This is due to the vortices generated by the wavy wall, which maintain a consistent conversion level.

In Fig. 11(a), distinct temperature extremes are evident. The minimum temperature is approximately 12  $^{\circ}$ C, due to the cooling jacket's effect. Meanwhile, the maximum temperature remains below the critical point of 75  $^{\circ}$ C, which is the permissible upper limit. This adherence to the maximum allowable temperature indicates effective temperature control within the system, which is crucial for maintaining safe operating conditions.

Examining various activation energy levels reveals an interesting trend in the conversion rate of propylene oxide. Notably, as the activation energy decreases, the conversion rate consistently increases. This trend culminates in a maximum conversion rate of 100 % and an average of 97 % when the activation energy is set at  $E = 74 \, \text{kJ/mol}$ . This indicates a significant sensitivity of the conversion process to changes in activation energy, highlighting the complex interplay between reaction kinetics and energy parameters in the propylene oxide conversion system (see Fig. 11(b)).

Fig. 12 shows the velocity profile of fluid within a cylindrical reactor at different axial positions (z = 0 to z = 1000 mm). The velocity magnitude is plotted against the reactor's radial coordinate (r), with a radius of 120 mm. The shaded area represents the cool-

ing jacket, ranging from 100 mm to 120 mm radius. The velocity profile is approximately uniform across different axial positions but decreases near the wall of the cooling jacket.

The wavy patterns in the velocity contour lines directly illustrate how the corrugated cooling jacket affects the flow (see Fig. 13). The fluid is forced to change direction and flow non-uniformly due to the corrugated inner wall. The closed loops visible in the contour plot indicate vortex formation in the spaces between the corrugations as the fluid navigates around these obstacles. The velocity contours show the fluid accelerating near the center of the reactor, likely due to the geometry of the reactor and the fluid being pushed through narrower spaces between the corrugations. The tighter contours near the corrugated wall indicate that the velocity slows down as it passes by the wall, suggesting some degree of boundary layer formation.

#### 4. Conclusions

This study has clarified the complex dynamics of reactor performance, thermal behavior, and conversion rates in propylene oxide conversion. The key contributions of this work include:

The data analysis has highlighted the critical impact of temperature variations and activation energy on conversion rates. Specifically, it was found that at an activation energy of E = 74 kJ/mol, the conversion rate reached a maximum of 100 %, with an average value of 97 %. This underscores the sensitivity of the system to activation energy and its importance in optimizing the conversion process.

The study has revealed that reactor conditions, such as initial temperature and activation energy, affect the exothermic reactions and are crucial for managing heat transfer dynamics within the reactor.

The study highlighted the cooling jacket's role in controlling temperature, showing how it helps maintain the right temperature and manage the heat released from reactions for better reactor performance.

The complexities of fluid flow, heat transfer, and fluid-structure interactions within the reactor were considered. Notably, the presence of vortices generated by corrugations in the reactor design promoted better mixing and improved conversion rates. The corrugated design was shown to enable nearly 100 % conversion of propylene oxide under optimal conditions by effectively managing the exothermic heat release.

While this research provides valuable insights into the potential of corrugated cooling jackets for propylene oxide decomposition, future investigations could explore various aspects to further enhance the process. These future directions could include examining the impact of different corrugated geometries, such as varying heights, widths, and spacings, on heat transfer, flow patterns, and conversion rates.

## CRediT authorship contribution statement

Djelloul Bendaho: Writing – review & editing, Writing – original draft, Methodology, Investigation, Conceptualization. Noureddine Kaid: Writing – review & editing, Writing – original draft, Methodology, Investigation, Conceptualization. Sultan Alqahtani: Writing – review & editing, Writing – original draft, Methodology, Investigation, Conceptualization. Badr M. Alshammari: Writing – review & editing, Writing – original draft, Methodology, Investigation, Conceptualization. Younes Menni: Writing – review & editing, Writing – original draft, Methodology, Investigation, Conceptualization. Ali J. Chamkha: Writing – review & editing, Writing – original draft, Methodology, Investigation, Conceptualization. Lioua Kolsi: Writing – review & editing, Writing – original draft, Methodology, Investigation, Conceptualization.

## **Declaration of competing interest**

The authors declare that they have no known competing financial interests or personal relationships that could have appeared to influence the work reported in this paper.

#### Acknowledgments

The authors extend their appreciation to the Deanship of Research and Graduate Studies at King Khalid University for funding this work through Large Research Project under grant number RGP2/352/45.

#### Data availability

Data will be made available on request.

#### References

- [1] A.G. Dixon, M. Nijemeisland, E.H. Stitt, Packed tubular reactor modeling and catalyst design using computational fluid dynamics, Adv. Chem. Eng. 31 (2006) 307–389, https://doi.org/10.1016/S0065-2377(06)31005-8.
- [2] M. Ahmed, R.W. Fahien, Tubular reactor design—I Two dimensional model, Chem. Eng. Sci. 35 (4) (1980) 889–895, https://doi.org/10.1016/0009-2509(80) 85076-7.
- [3] F.A. Cleland, R.H. Wilhelm, Diffusion and reaction in viscous-flow tubular reactor, AIChE J. 2 (4) (1956) 489-497, https://doi.org/10.1002/aic.690020414.
- [4] O. Awogbemi, D.V.V. Kallon, Application of tubular reactor technologies for the acceleration of biodiesel production, Bioengineering 9 (8) (2022) 347, https://doi.org/10.3390/bioengineering9080347.
- [5] M.L. Goldberger, K.M. Watson, Collision theory, Courier Corporation (2004) 919.
- [6] M.S. Child, Molecular collision theory, Courier Corporation (2014) 310.
- [7] D. Stoianovici, Y. Hurmuzlu, A critical study of the applicability of rigid-body collision theory, J. Appl. Mech. 63 (2) (1996) 307–316, https://doi.org/10.1115/

#### 1 2788865

- [8] A.A. Memon, M.A. Memon, K. Bhatti, I. Khan, N. Alshammari, A.S. Al-Johani, N.N. Hamadneh, M. Andualem, Thermal decomposition of propylene oxide with different activation energy and Reynolds number in a multicomponent tubular reactor containing a cooling jacket, Sci. Rep. 12 (1) (2022) 4169, https://doi.org/ 10.1038/s41598.022-06481-4
- [9] T. Ozawa, Estimation of activation energy by isoconversion methods, Thermochim. Acta 203 (1992) 159–165, https://doi.org/10.1016/0040-6031(92)85192-
- [10] J. Jortner, Temperature dependent activation energy for electron transfer between biological molecules, J. Chem. Phys. 64 (12) (1976) 4860–4867, https://doi.org/10.1063/1.432142
- [11] D.G. Truhlar, Interpretation of the activation energy, J. Chem. Educ. 55 (5) (1978) 309, https://doi.org/10.1021/ed055p309.
- [12] J.C.H. Célestin, M. Fall, Thermal conductivity of cemented paste backfill material and factors affecting it, Int. J. Min. Reclamat. Environ. 23 (4) (2009) 274–290, https://doi.org/10.1080/17480930902731943.
- [13] K. Cacua, S.S. Murshed, E. Pabón, R. Buitrago, Dispersion and thermal conductivity of TiO<sub>2</sub>/water nanofluid: effects of ultrasonication, agitation and temperature, J. Therm. Anal. Calorim. 140 (2020) 109–114.
- [14] A. Maleki, A. Haghighi, M. Irandoost Shahrestani, Z. Abdelmalek, Applying different types of artificial neural network for modeling thermal conductivity of nanofluids containing silica particles, J. Therm. Anal. Calorim. 144 (2021) 1613–1622, https://doi.org/10.1007/s10973-020-09541-x.
- [15] M. Awais, N. Ullah, J. Ahmad, F. Sikandar, M.M. Ehsan, S. Salehin, A.A. Bhuiyan, Heat transfer and pressure drop performance of Nanofluid: a state-of-the-art review, International Journal of Thermofluids 9 (2021) 100065, https://doi.org/10.1016/j.ijft.2021.100065.
- [16] J. Keizer, Diffusion effects on rapid bimolecular chemical reactions, Chem. Rev. 87 (1) (1987) 167–180, https://doi.org/10.1021/cr00077a009.
- [17] D. Ben-Avraham, S. Havlin, Diffusion and Reactions in Fractals and Disordered Systems, Cambridge University Press, 2000, p. 316.
- [18] R.I. Masel, Chemical Kinetics and Catalysis, vol. 10, Wiley-Interscience, New York, 2001.
- [19] U.N. Das, R. Deka, V.M. Soundalgekar, Effects of mass transfer on flow past an impulsively started infinite vertical plate with constant heat flux and chemical reaction, Forsch. Im. Ingenieurwes. 60 (10) (1994) 284–287, https://doi.org/10.1007/BF02601318.
- [20] N.M. Brown, F.C. Lai, Correlations for combined heat and mass transfer from an open cavity in a horizontal channel, Int. Commun. Heat Mass Tran. 32 (8) (2005) 1000–1008, https://doi.org/10.1016/j.icheatmasstransfer.2004.10.029.
- [21] S. Parvin, R. Nasrin, M.A. Alim, N.F. Hossain, Double-diffusive natural convection in a partially heated enclosure using a nanofluid, Heat Tran. Asian Res. 41 (6) (2012) 484–497, https://doi.org/10.1002/htj.21010.
- [22] V. Rajesh, MHD and chemical reaction effects on free convection flow with variable temperature and mass diffusion, Annals-Journal of Engineering, Tome VIII (year 2010), Fascicule 3 (2010) 370–378.
- [23] A.J. Chamkha, MHD flow of a uniformly stretched vertical permeable surface in the presence of heat generation/absorption and a chemical reaction, Int. Commun. Heat Mass Tran. 30 (3) (2003) 413–422, https://doi.org/10.1016/S0735-1933(03)00059-9.
- [24] F.S. Ibrahim, A.M. Elaiw, A.A. Bakr, Effect of the chemical reaction and radiation absorption on the unsteady MHD free convection flow past a semi infinite vertical permeable moving plate with heat source and suction, Commun. Nonlinear Sci. Numer. Simulat. 13 (6) (2008) 1056–1066, https://doi.org/10.1016/j.cnsns.2006.09.007.
- [25] R.A. Mohamed, S.M. Abo-Dahab, Influence of chemical reaction and thermal radiation on the heat and mass transfer in MHD micropolar flow over a vertical moving porous plate in a porous medium with heat generation, Int. J. Therm. Sci. 48 (9) (2009) 1800–1813, https://doi.org/10.1016/j.ijthermalsci.2009.01.019.
- [26] D.C. Kesavaiah, P.V. Satyanarayana, S. Venkataramana, Effects of the chemical reaction and radiation absorption on an unsteady MHD convective heat and mass transfer flow past a semi-infinite vertical permeable moving plate embedded in a porous medium with heat source and suction, Int. J. Appl. Math. Mech. 7 (1) (2011) 52–69
- [27] T. Hayat, M. Rashid, A. Alsaedi, Three dimensional radiative flow of magnetite-nanofluid with homogeneous-heterogeneous reactions, Results Phys. 8 (2018) 268–275, https://doi.org/10.1016/j.rinp.2017.11.038.
- [28] G. Ribert, N. Zong, V. Yang, L. Pons, N. Darabiha, S. Candel, Counterflow diffusion flames of general fluids: oxygen/hydrogen mixtures, Combust. Flame 154 (3) (2008) 319–330, https://doi.org/10.1016/j.combustflame.2008.04.023.
- [29] N. Bachok, A. Ishak, I. Pop, On the stagnation-point flow towards a stretching sheet with homogeneous–heterogeneous reactions effects, Commun. Nonlinear Sci. Numer. Simulat. 16 (11) (2011) 4296–4302, https://doi.org/10.1016/j.cnsns.2011.01.008.
- [30] S.V. Frolov, A.A. Tret'yakov, V.N. Nazarov, Problem of optimal control of monomethylaniline synthesis in a tubular reactor, Theor. Found. Chem. Eng. 40 (4) (2006) 349–356, https://doi.org/10.1134/S0040579506040038.
- [31] M.E. Masoumi, S.M. Sadrameli, J. Towfighi, A. Niaei, Simulation, optimization and control of a thermal cracking furnace, Energy 31 (4) (2006) 516–527, https://doi.org/10.1016/j.energy.2005.04.005.
- [32] S.A. Logtenberg, A.G. Dixon, Computational fluid dynamics studies of fixed bed heat transfer, Chem. Eng. Process: Process Intensif. 37 (1) (1998) 7–21, https://doi.org/10.1016/S0255-2701(97)00032-9.
- [33] R. Kusumastuti, P.C. Cheng, C.J. Tseng, A numerical study of internally heating, counter-flow tubular packed bed reactor for methanol steam reforming, Int. J. Hydrogen Energy 52 (2024) 964–977, https://doi.org/10.1016/j.ijhydene.2023.04.187.
- [34] B.C. Nailwal, P. Chotalia, J. Salvi, N. Goswami, L. Muhmood, A.K. Adak, S. Kar, Ammonia decomposition for hydrogen production using packed bed catalytic membrane reactor, Int. J. Hydrogen Energy 49 (2024) 1272–1287, https://doi.org/10.1016/j.ijhydene.2023.09.229.
- [35] Z. Wu, Z. Guo, J. Yang, Q. Wang, Numerical investigation of hydrogen production via methane steam reforming in a novel packed bed reactor integrated with diverging tube, Energy Convers. Manag. 289 (2023) 117185, https://doi.org/10.1016/j.enconman.2023.117185.

## NomenclatureSymboleDefinition Unit

- $D_P$ : Diffusivity of the substance  $C_A$  in the medium  $m^2/s$
- $C_A$ : Concentration of species A mol/m
- $\frac{dT}{dX}$ : Temperature gradient K/m
- E: Reaction activation energy J/mol
- K: Thermal conductivity W/(m.K)
- k: Reaction rate 1/s
- $k_0$ : Pre-exponential factor 1/s
- L: Length m
- R: Universal gas constant J/(K.mol)
- $R_a$ : Radius of the cylindrical system m
- r: Radial coordinate m
- $r_A$ : Reaction rate of species A mol/(m<sup>3</sup>.s)
- *T*: Absolute temperature K
- $T_0$ : Reference temperature K
- U: Velocity in the axial direction z m/s
- $U_K$ : Overall heat transfer coefficient W/m<sup>2</sup>.K
- ρ: Density Kg/m<sup>3</sup>